Standing waves on two-dimensional periodic dielectric waveguides

Zhen Hu[1] and Ya Yan Lu[2]

[1]*Department of Mathematics, Hohai University, Nanjing, Jiangsu, China*
[2]*Department of Mathematics, City University of Hong Kong, Kowloon, Hong Kong*

compiled: March 26, 2015

Guided modes of a periodic waveguide usually exist below the light line, if the minimum period of the waveguide is used in the definition, but for some periodic waveguides, there are standing waves with the same period as the waveguide. These non-propagating waves localized around the waveguide core are special guided modes above the light line with a zero wavenumber, and they are related to transmission anomalies and other resonant phenomena. In this paper, we analyze the standing waves on two periodic waveguides: a periodic array of circular dielectric cylinders, and a dielectric slab with a periodic array of circular air-holes. Based on an efficient semi-analytic method, the frequencies of standing waves are calculated as functions of the dielectric constant and the radius of cylinders. Our work provides a basis for further studies on these waves and for realizing their potential applications.

1. Introduction

Waveguides with a periodic structural variation along their axes appear in various forms and have been analyzed by many authors [1–5]. On a lossless periodic waveguide, a genuine guided mode is a Bloch wave with a real wavenumber β and a periodic mode profile that decays exponentially away from the waveguide core. If the periodic waveguide is surrounded by a homogeneous medium with dielectric constant ε_0, then guided modes usually only exist below the light line, i.e., they satisfy $k_0\sqrt{\varepsilon_0} < |\beta|$, where k_0 is the free space wavenumber. Above the light line is a continuum of radiation modes, thus the wave field is unlikely to be confined around the waveguide core. In that case, it is useful to find guided resonances [6, 7] which have a real β and a complex ω (the angular frequency). The imaginary part of ω gives the decay rate of the wave field with time. Alternatively, we can look for leaky waveguide modes with a real ω and complex β. Such a leaky mode decays as it propagates along the waveguide. For both guided resonances and leaky waveguide modes, the field exhibits outgoing wave behavior in the transverse plane perpendicular to the waveguide axis, and it blows up at infinity.

Actually, true guided modes that decay exponentially away from the waveguide core could exist above the light line in periodic waveguides [8–19]. Notice that if the waveguide is periodic along it axis, we need to use its minimum period a. Otherwise, due to band folding, a guided mode below the light line for a waveguide with period a, could become a mode above the light line for a waveguide with period ma, where $m > 1$ is an integer. For example, a guided mode below the light line with $\beta = \pi/a$ (the end point of the first Brillouin zone), can be regarded as a mode with $\beta = 0$ for a waveguide with period $2a$. When the minimum period of the waveguide is used, guided modes above the light line typically only exist for isolated pairs of β and ω, since a small perturbation in the waveguide geometry or material parameters can easily excite the radiation modes, making field confinement around the waveguide core impossible. Near such a non-robust guided mode, as the wavenumber of a guided resonance tends to that of the guided mode, the imaginary part of ω tends to zero, thus the lifetime and the quality factor of the resonance mode tend to infinity. External plane waves can interact with the nearby guided resonances, leading to arbitrarily large field intensities around the waveguide, and the transmission spectra could have anomalies with arbitrarily close total and zero extremum points [20, 21]. The enhanced lifetime and strong field localization near these standing waves suggest potential applications in sensing, lasing, fluorescence enhancement, nonlinear photonics, etc, where a strong light-matter interaction is desired.

For guided modes above the light line, some existence theories and some examples are available [8, 12]. Most existing examples are related to the special case $\beta = 0$ which corresponds to standing waves. It appears that a systematic study on guided modes above the light line is highly desired and currently not available. In this paper, we analyze two simple two-dimensional (2D) periodic waveguides: a periodic array of circular dielectric cylinders and a dielectric slab with a periodic array of circular holes. We calculate the standing waves for these two periodic waveguides, determine their dependency on geometric parameters and the dielectric constant of the medium. To take advantage of the circular geometry of the dielectric cylinders and air-holes, we develop a special semi-analytic method that relies on cylindrical wave expansions and a formulation involving very small matrices.

2. Standing waves and their computation

We consider two simple 2D periodic waveguides. The first waveguide, shown in Fig. 1(a), is a periodic array

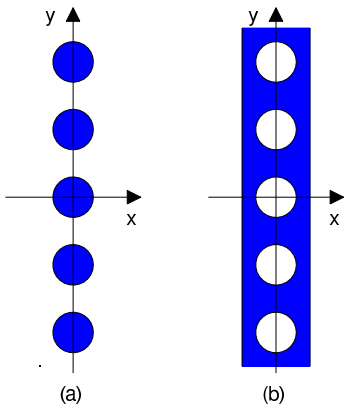

Fig. 1. Two periodic waveguides: (a) a periodic array of dielectric cylinders; (b) a dielectric slab with a periodic array of air-holes.

of infinitely long and parallel dielectric circular cylinders surrounded by air. The period of the array, i.e., the center-to-center distance of nearby cylinders, is a. The radius and the dielectric constant of the cylinders are r and ε_1, respectively. The second waveguide, shown in Fig. 1(b), is a dielectric slab with a periodic array of circular air-holes of radius r. The thickness of the slab and the period of the array are both a. The slab is surrounded by air and its dielectric constant is ε_1. A Cartesian coordinate system $\{x, y, z\}$ is chosen, such that the dielectric cylinders or the air-holes are parallel to the z axis, their centers are located on the y axis at $y = ja$ for all integers j. Notice that the origin is at the center of one cylinder or air-hole. Clearly, these waveguides are periodic in y with the period a, and are symmetric with respect to x and y axes.

Since the structures are z-invariant, if the wave field is also z-invariant, we can consider two separate polarizations. For the E-polarization, the governing equation is the Helmholtz equation

$$\frac{\partial^2 u}{\partial x^2} + \frac{\partial^2 u}{\partial y^2} + k_0^2 \varepsilon\, u = 0, \tag{1}$$

where u is the z component of the electric field, $\varepsilon = \varepsilon(x, y)$ is the dielectric function that takes the values ε_1 or $\varepsilon_0 = 1$ for the dielectric or air, respectively. For the H-polarization, the governing equation is a slightly different Helmholtz equation

$$\frac{\partial}{\partial x}\left(\frac{1}{\varepsilon}\frac{\partial u}{\partial x}\right) + \frac{\partial}{\partial y}\left(\frac{1}{\varepsilon}\frac{\partial u}{\partial y}\right) + k_0^2 u = 0, \tag{2}$$

where u is the z component of the magnetic field.

A guided mode on such a periodic waveguide is a Bloch wave given as

$$u(x, y) = \phi(x, y) e^{i\beta y}, \tag{3}$$

where the Bloch wavenumber β is real, and the mode profile ϕ is periodic in y with period a and decays to zero exponentially as $x \to \pm\infty$. Due to the periodicity of ϕ, it is only necessary to consider β in the first Brillouin zone, i.e., $-\pi/a \le \beta \le \pi/a$. Usually, the guided modes appear below the light line, that is, k_0 and β satisfy $k_0\sqrt{\varepsilon_0} < |\beta|$.

Since ϕ is periodic in y, it can be expanded in Fourier series. This leads to the following expansion:

$$u(x, y) = \begin{cases} \sum c_m^- e^{i(\beta_m y - \alpha_m x)}, & x < -a/2, \\ \sum c_m^+ e^{i(\beta_m y + \alpha_m x)}, & x > a/2, \end{cases} \tag{4}$$

where m goes over all integers, and

$$\beta_m = \beta + \frac{2\pi m}{a}, \quad \alpha_m = \sqrt{k_0^2\varepsilon_0 - \beta_m^2}. \tag{5}$$

In the above, if $k_0^2\varepsilon_0 - \beta_m^2 < 0$, then $\alpha_m = i\sqrt{\beta_m^2 - k_0^2\varepsilon_0}$. For a guided mode below the light line and $|\beta| \le \pi/a$, it is clear that all α_m are pure imaginary, and thus u decays to zero as $x \to \pm\infty$. Above the light line, α_0 and may be a few other α_m are real and positive, therefore, a guided mode can only exist when $c_0^\pm = 0$ and other $c_m^\pm = 0$ if $\alpha_m > 0$. These conditions are not satisfied in general, therefore guided modes above the light line are more difficult to find.

For a standing wave ($\beta = 0$) in the lowest frequency range given by $k_0 < 2\pi/(a\sqrt{\varepsilon_0})$, we have $\alpha_0 > 0$ and all other α_m for $m \neq 0$ are pure imaginary. Therefore, the only condition for this case is $c_0^\pm = 0$. Notice that if u is an odd function of y, i.e., $u(x, -y) = -u(x, y)$, then $c_0^\pm = 0$ is guaranteed. The waveguides shown in Fig. 1 have a reflection symmetry with respect to the x axis (more precisely, the xz plane), thus, the dielectric function ε is an even function of y, i.e., $\varepsilon(x, -y) = \varepsilon(x, y)$. For general symmetric periodic waveguides, the existence of standing waves can be rigorously proved [8, 12]. A brief outline of the proof is given in Appendix A.

To find the standing waves, we need to solve an eigenvalue problem in one period of the waveguide, i.e., in the trip given by $|y| < a/2$, for Eq. (1) or Eq. (2), with a periodic boundary condition in the y direction, and the condition $u \to 0$ as $x \to \pm\infty$. The eigenvalue is k_0^2. For symmetric waveguides, if we look for odd standing waves, then the problem can be solved in one half of the period, i.e., for $0 < y < a/2$, with zero boundary conditions $u = 0$ at $y = 0$ and $y = a/2$. The waveguides shown in Fig. 1 are also symmetric with respect to the y axis, i.e., $\varepsilon(x, y) = \varepsilon(-x, y)$. Therefore, the computational domain can be further reduced by one half, i.e., for $x > 0$ only, if we separately consider standing waves that are even or odd in x, with the corresponding boundary conditions $\partial_x u = 0$ or $u = 0$ at $x = 0$.

For the two waveguides shown in Fig. 1, we can develop a more efficient semi-analytic method by taking advantage of the circular geometry of the dielectric cylinders and air-holes. For that purpose, we first formulate the problem on the square Ω given by $|x| < a/2$ and

$|y| < a/2$, and find proper conditions on the boundary of Ω. Let us consider the E-polarization first. Since u is a standing wave, it is periodic in y, therefore,

$$u(x, -a/2) = u(x, a/2), \tag{6}$$

$$\frac{\partial u}{\partial y}(x, -a/2) = \frac{\partial u}{\partial y}(x, a/2). \tag{7}$$

Since u has a plane wave expansion (4) for $|x| > a/2$, we can define a linear operator $\boldsymbol{T}$ such that

$$\boldsymbol{T}\, e^{i\beta_m y} = i\alpha_m\, e^{i\beta_m x} \quad \text{for all} \quad m, \tag{8}$$

then

$$\frac{\partial u}{\partial x} = \pm \boldsymbol{T} u, \quad x = \pm\frac{a}{2}. \tag{9}$$

Notice that $\boldsymbol{T}$ depends on k_0. For a given k_0, if each edge of the square Ω is discretized by N points, then $\boldsymbol{T}$ can be approximated by an $N \times N$ square matrix.

Inside Ω, u satisfies Eq. (1) and it has a cylindrical wave expansion. Although the expansion coefficients are unknown, we can use this expansion to write down $\partial_x u$ and $\partial_y u$. This leads to a linear relation $\boldsymbol{\Lambda}$, the so-called Dirichlet-to-Neumann (DtN) map, between u and its normal derivatives on the boundary of Ω [22, 23], such that

$$\boldsymbol{\Lambda} \begin{bmatrix} u(-a/2, y) \\ u(x, -a/2) \\ u(a/2, y) \\ u(x, a/2) \end{bmatrix} = \begin{bmatrix} \partial_x u(-a/2, y) \\ \partial_y u(x, -a/2) \\ \partial_x u(a/2, y) \\ \partial_y u(x, a/2) \end{bmatrix}. \tag{10}$$

Using N points on each edge of Ω, the operator $\boldsymbol{\Lambda}$ can be approximated by a $(4N) \times (4N)$ matrix [22, 23]. From Eqs. (6), (7), (9) and (10), we can make some eliminations and obtain a $(3N) \times (3N)$ homogeneous linear system

$$\boldsymbol{A} \begin{bmatrix} u(-a/2, y) \\ u(x, -a/2) \\ u(a/2, y) \end{bmatrix} = 0. \tag{11}$$

Since both $\boldsymbol{T}$ and $\boldsymbol{\Lambda}$ depend on k_0, the matrix $\boldsymbol{A}$ also depends on k_0. Actually, k_0 is the unknown wavenumber of a standing wave. Therefore, we determine k_0 from the condition that $\boldsymbol{A}$ is a singular matrix, so that a nontrivial solution for u exists. In practice, we search k_0 by solving

$$\sigma_1(\boldsymbol{A}) = 0, \tag{12}$$

where σ_1 is the smallest singular value of the matrix $\boldsymbol{A}$ [24]. The method is semi-analytic, since the operator $\boldsymbol{\Lambda}$ is constructed from a cylindrical wave expansion of u. Since the size of matrix $\boldsymbol{A}$ can be very small, the method is efficient.

For the H-polarization and the second waveguide shown in Fig. 1(b), the lines $x = \pm a/2$ are the interfaces between the slab and air. The definition of $\boldsymbol{T}$ is unchanged, but the boundary conditions (9) are valid at $x = (a/2)^+$ and $x = -(a/2)^-$, respectively. The DtN map $\boldsymbol{\Lambda}$ for Eq. (2) can be similarly constructed, but $\partial_x u$ in the right hand side of (10) must be evaluated at $x = -(a/2)^+$ or $x = (a/2)^-$. To obtain the final linear system (11), it is necessary to use the following matching conditions

$$\frac{1}{\varepsilon_0}\frac{\partial u}{\partial x}\bigg|_{x=-(a/2)^-} = \frac{1}{\varepsilon_1}\frac{\partial u}{\partial x}\bigg|_{x=-(a/2)^+},$$

$$\frac{1}{\varepsilon_1}\frac{\partial u}{\partial x}\bigg|_{x=(a/2)^-} = \frac{1}{\varepsilon_0}\frac{\partial u}{\partial x}\bigg|_{x=(a/2)^+}.$$

3. Results

Based on the method presented in the previous section, we analyze standing waves on the two waveguides shown in Fig. 1. For the periodic array of dielectric cylinders, we consider the E-polarization, and first calculate the standing wave with the lowest frequency for different values of r and ε_1. The results are shown in Fig. 2 (top panel). The frequency is given as functions of the dielectric constant ε_1 for radius $r = 0.1a$, $0.15a$, $0.2a$, ..., $0.45a$. We observe that the frequency tend to be smaller for cylinders with a larger radius. At a lower frequency, the cylinders must have a larger dielectric constant to

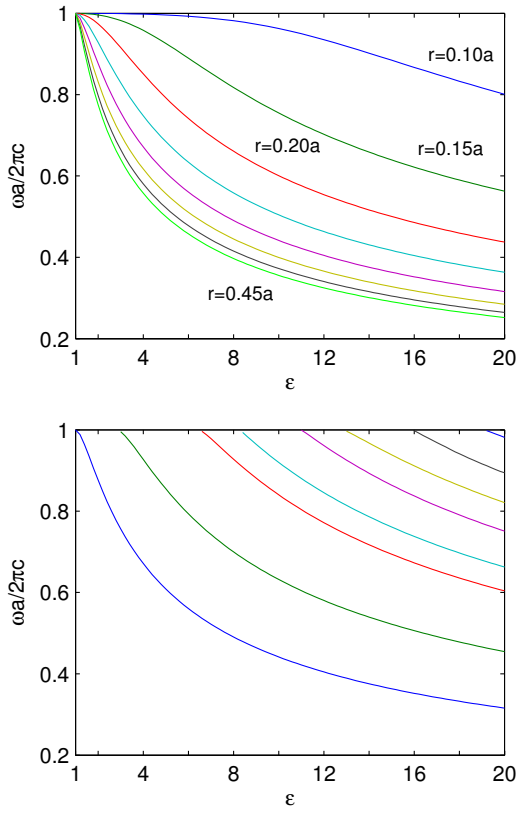

Fig. 2. Top: Standing wave with the smallest frequency on periodic arrays of circular cylinders with radius r and dielectric constant ε_1. Bottom: Frequencies of all standing waves on an array of circular cylinders with radius $r = 0.3a$.

support a standing wave. The curves terminate at $\varepsilon_1 = 1$ and $k_0 a/(2\pi) = \omega a/(2\pi c) = 1$, where c is the speed of light in vacuum. We restrict ourself to the frequency range $\omega a/(2\pi c) \leq 1$. Even in this range, depending on the radius and the dielectric constant of the cylinders, there may be many standing waves. In Fig. 2 (bottom panel), we show the frequencies of all standing waves for a fixed radius $r = 0.3a$. For $\varepsilon_1 = 20$, there are eight standing waves. As ε_1 is decreased, these standing waves disappear one by one all at $\omega a/(2\pi c) = 1$. This is related to the fact that when $\omega a/(2\pi c) > 1$, α_1 and α_{-1} become real, but the coefficients $c_1^{\pm}$ and $c_{-1}^{\pm}$ in (4) are nonzero in general. For $\varepsilon_1 = 11.6$, there are five standing waves with frequencies $\omega a/2\pi c = 0.4112$, 0.5897, 0.7842, 0.8590, and 0.9766. The electric field patterns of these standing waves are shown in Fig. 3. As mentioned earlier, the waveguide is symmetric with respect to the x axis, but the standing waves are anti-symmetric, i.e., u is an odd function of y. As a result, the Fourier coefficients $c_0^{\pm}$ are zero. In fact, we have $u = 0$ on the x-axis, and also on the two horizontal lines at $y = \pm a/2$. With respect to the y-axis, the electric field is either symmetric (even function of x) or anti-symmetric (odd function of x) as shown in Fig. 3. These results are obtained using $N = 5$ points on each edge of the square Ω, therefore, the size of matrix $\boldsymbol{A}$ is just 15×15.

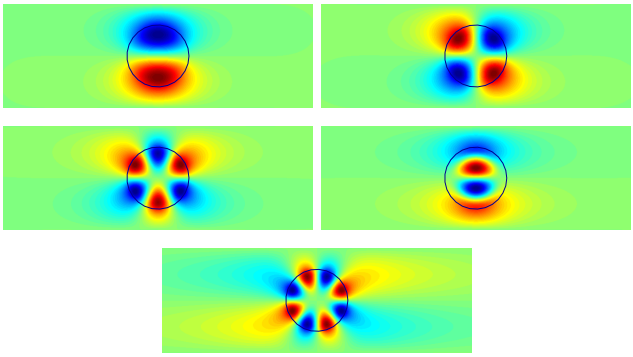

Fig. 3. Electric field patterns of the five standing waves on a periodic array of cylinders with $r = 0.30a$ and $\varepsilon_1 = 11.6$. The frequencies are $\omega a/2\pi c = 0.4112$, 0.5897, 0.7842, 0.8590, and 0.9766.

For the dielectric slab with an array of air-holes, we consider the H polarization and assume $r = 0.3a$, where a is the period of the array and the thickness of the slab, and r is the radius of the air-holes. When the dielectric constant of the slab ε_1 is large, there are many standing waves with their frequencies satisfying $\omega a/(2\pi c) < 1$. In Fig. 4, we show these frequencies as functions of ε_1. Similar to the first waveguide, standing waves exist whenever $\varepsilon_1 > 1$ and disappear at $\omega a/(2\pi c) = 1$. Meanwhile, as ε_1 is increased, the frequency of each standing wave decreases, and the total number of standing waves increases. For $\varepsilon_1 = 11.6$, there are nine standing waves within the above frequency range. In Fig. 5, we show their magnetic field patterns. As expected, all these nine

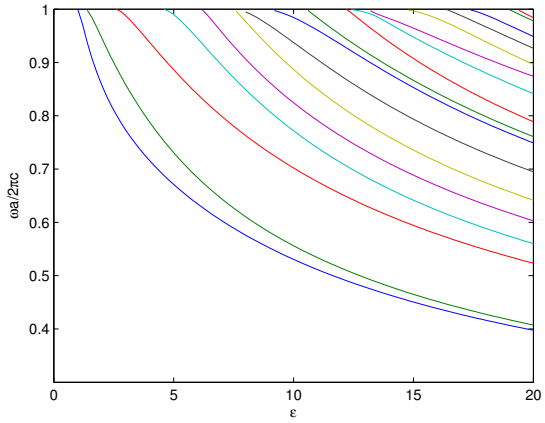

Fig. 4. Frequencies of standing waves on a dielectric slab with an array of air-holes of radius $r = 0.3a$.

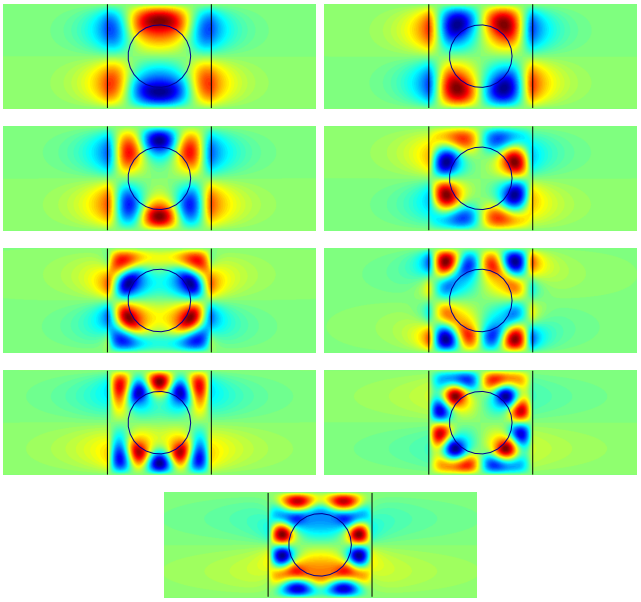

Fig. 5. Magnetic field patterns of the nine standing waves on a slab ($\varepsilon_1 = 11.6$) with an array of air-holes.

modes are anti-symmetric with respect to the x axis, and they can be either symmetric or anti-symmetric with respect to the y axis. In fact, it is clear that $u = 0$ on the horizontal lines at $y = 0$ and $y = \pm a/2$. It can also be seen that the magnetic field of every mode reaches its largest magnitude in the slab region. These results are obtained with $N = 9$ points on each edge of the square Ω, therefore, $\boldsymbol{A}$ is a 27×27 matrix.

4. Conclusion

For lossless periodic waveguides, guided modes defined based on the minimum period, usually only exist below the light line, but for waveguides with a reflection symmetry along its axis, standing waves having a zero Bloch wavenumber (and clearly above the light line) exist un-

der rather general conditions [8, 12]. These standing waves are non-robust, they give rise to nearby guided resonances with lifetime and quality factor tending to infinity, and are related to interesting transmission anomalies [20, 21]. Since there are few published examples for standing waves on periodic waveguides, we perform a detailed study for a periodic array of dielectric cylinders and a periodic array of air-holes in a dielectric slab. For these two periodic waveguides, we calculate the standing waves based on an efficient computational method, and show their dependence on the material and geometric parameters. Our work provides a starting point for further studies on standing waves and guided modes above the light line, and can be useful for realizing practical applications of these special guided waves.

Acknowledgment

This work was supported by the National Natural Science Foundation of China under project 11101122, and the Research Grants Council of Hong Kong Special Administrative Region, China, under project CityU 102411.

Appendix A

Consider a waveguide that is periodic in y with a minimum period a and symmetric about the x axis, i.e., $\varepsilon(x,y)=\varepsilon(x,-y)$. We show that anti-symmetric (i.e., $u(x,-y)=-u(x,y)$) standing waves exist within the frequency range $k_0<2\pi/(a\sqrt{\varepsilon_0})$. In one-half of the period

$$S=\{(x,y)\ :\ -\infty<x<\infty,\, 0<y<a/2\},$$

the dielectric function satisfies $\varepsilon=\varepsilon_1$ in a bounded domain Σ and $\varepsilon=\varepsilon_0$ in the exterior of Σ, where ε_1 could be a function of x and y, and $\varepsilon_1>\varepsilon_0$. For the E polarization, the anti-symmetric standing waves are the solutions of the eigenvalue problem satisfying Eq. (1) in S and the following boundary conditions

$$u(x,0)=u(x,a/2)=0, \tag{13}$$
$$\lim_{x\to\pm\infty} u(x,y)=0, \tag{14}$$

where k_0^2 is the eigenvalue. For any $k_0^2\geq\lambda_*=(2\pi)^2/(\varepsilon_0 a^2)$, Eq. (1) has solutions that satisfy the boundary condition (13) and are bounded by $O(|x|^m)$ for some integer $m\geq 0$ as $|x|\to\infty$. In particular, for $k_0^2>\lambda_*$, there is a solution associated with the scattering problem of the incident wave $u^{(i)}=\sin(2\pi y/a)e^{i\alpha x}$, where $\alpha=[k_0^2\varepsilon_0-(2\pi/a)^2]^{1/2}>0$, and the solution is bounded as $x\to\pm\infty$. This leads to the conclusion that the continuous spectrum of the eigenvalue problem is the semi-infinite interval $[\lambda_*,\infty)$ [25, 26]. If k_0^2 is an eigenvalue and u is the corresponding eigenfunction for eigenvalue problem (1), (13) and (14), it is easily shown that

$$k_0^2=\frac{\int_S|\nabla u|^2\mathrm{d}x\mathrm{d}y}{\int_S\varepsilon|u|^2\mathrm{d}x\mathrm{d}y}. \tag{15}$$

On the other hand, let H_0^1 be the space of functions on S that satisfy the boundary condition (13), are square-integrable, and their gradients are square-integrable, we can consider the problem

$$\lambda_{min}=\inf_{\psi\in H_0^1}\frac{\int_S|\nabla\psi|^2\mathrm{d}x\mathrm{d}y}{\int_S\varepsilon|\psi|^2\mathrm{d}x\mathrm{d}y}. \tag{16}$$

If $\lambda_{min}<\lambda_*$, then λ_{min} is the smallest eigenvalue of the above eigenvalue problem [25, 26]. In that case, there is at least one standing wave with a wavenumber $k_0=(\lambda_{min})^{1/2}$.

To show that $\lambda_{min}<\lambda_*$, it is only necessary to find one specific function Ψ, such that

$$\frac{\int_S|\nabla\Psi|^2\mathrm{d}x\mathrm{d}y}{\int_S\varepsilon|\Psi|^2\mathrm{d}x\mathrm{d}y}<\lambda_*. \tag{17}$$

Let $G(\tau)$ be a smooth function, such that $G(\tau)=1$ for $|\tau|\leq 1$ and $G(\tau)=0$ for $|\tau|\geq 2$. We define a function Ψ (depending on a parameter $S>0$) by

$$\Psi(x,y)=\sin(2\pi y/a)\,G(x/S), \tag{18}$$

then straightforward calculations lead to

$$\begin{aligned}&\lambda_*\int_S\varepsilon|\Psi|^2\mathrm{d}x\mathrm{d}y-\int_S|\nabla\Psi|^2\mathrm{d}x\mathrm{d}y\\&=\lambda_*\int_\Sigma(\varepsilon_1-\varepsilon_0)\sin^2(2\pi y/a)\mathrm{d}x\mathrm{d}y-\frac{a}{4S}\int_{-2}^{2}|G'(\tau)|^2\mathrm{d}\tau.\end{aligned}$$

Since the first term is positive and the second term tends to zero as $S\to\infty$, it is clear that for a sufficiently large S, Eq. (17) is satisfied.

For the H-polarization, the eigenvalue problem consists of Eq. (2) and boundary conditions (13) and (14). The Rayleigh quotient formula (15) becomes

$$k_0^2=\frac{\int_S\frac{1}{\varepsilon}|\nabla u|^2\mathrm{d}x\mathrm{d}y}{\int_S|u|^2\mathrm{d}x\mathrm{d}y}. \tag{19}$$

Eq. (16) should be similarly modified, the same function Ψ can be used in the proof, and the proof is nearly identical.

References

[1] A. A. Oliner and A. Hessel, "Guided waves on sinusoidally-modulated reactance surfaces," IRE Trans. Antennas and Propagation **7**(5), S201-S208 (1959).

[2] S. Peng, T. Tamir, and H. Bertoni, "Theory of periodic dielectric waveguides," IEEE Trans. Microwave Theory Tech. **23**(1), 123-133 (1975).

[3] S. Fan, J. N. Winn, A. Devenyi, J. C. Chen, R. D. Meade, and J. D. Joannopoulos, "Guided and defect modes in periodic dielectric waveguides," J. Opt. Soc. Am. B **12**(7), 1267-1272 (1995).

[4] S. G. Johnson, P. R. Villeneuve, S. Fan, and J. D. Joannopoulos, "Linear waveguides in photonic-crystal slabs," Phys. Rev. B **62**, 8212-8222 (2000).

[5] D. N. Chigrin, A. V. Lavrinenko, and C. M. Sotomayor Torres, "Nanopillars photonic crystal waveguides," Opt. Express **12**, 617-622 (2004).

[6] R. Magnusson and S. S. Wang, "New principle for optical filters," Appl. Phys. Lett. **61**, 1022-1024 (1992).

[7] S. Fan and J. D. Joannopoulos, "Analysis of guided resonances in photonic crystal slabs," Phys. Rev. B **65**, 235112 (2002).

[8] A.-S. Bonnet-Bendhia and F. Starling, "Guided waves by electromagnetic gratings and nonuniqueness examples for the diffraction problem," Math. Methods Appl. Sci. **17**, 305–338 (1994).

[9] H. D. Maniar and J. N. Newman, "Wave diffraction by a long array of cylinders," J. Fluid Mech. **339**, 309–330 (1997).

[10] D. V. Evans and R. Porter, "Trapped modes embedded in the continuous spectrum," Q. J. Mech. Appl. Math. **51**(2), 263–274 (1998).

[11] R. Porter and D. V. Evans, "Embedded Rayleigh-Bloch surface waves along periodic rectangular arrays," Wave Motion **43**, 29–50 (2005).

[12] S. Shipman and D. Volkov, "Guided modes in periodic slabs: existence and nonexistence," SIAM J. Appl. Math. **67**, 687–713 (2007).

[13] D. C. Marinica, A. G. Borisov, and S. V. Shabanov, "Bound states in the continuum in photonics," Phys. Rev. Lett. **100**, 183902 (2008).

[14] Y. Plotnik, O. Peleg, F. Dreisow, M. Heinrich, S. Nolte, A. Szameit, and M. Segev, "Experimental observation of optical bound states in the continuum," Phys. Rev. Lett. **107**, 183901 (2011).

[15] M. I. Molina, A. E. Miroshnichenko, and Y. S. Kivshar, "Surface bound states in the continuum," Phys. Rev. Lett. **108**, 070401 (2012).

[16] J. Lee, B. Zhen, S. Chua, W. Qiu, J. D. Joannopoulos M. Soljačić, and O. Shapira, "Observation and differentiation of unique high-Q optical resonances near zero wave vector in macroscopic photonic crystal slabs," Phys. Rev. Lett. **109**, 067401 (2012).

[17] C. W. Hsu, B. Zhen, S.-L. Chua, S. G. Johnson, J. D. Joannopoulos, and M. Soljačić, "Bloch surface eigenstates within the radiation continuum," Light: Science & Applications **2**, e84 (2013).

[18] C. W. Hsu, B. Zhen, J. Lee, S.-L. Chua, S. G. Johnson, J. D. Joannopoulos, and M. Soljačić, "Observation of trapped light within the radiation continuum," Nature **499**, 188-191 (2013).

[19] B. Zhen, C. W. Hsu, L. Lu, A. D. Stone, and M. Soljačić, "Topological nature of optical bound states in the continuum," Phys. Rev. Lett. **113**, 257401 (2014).

[20] S. Shipman and S. Venakides, "Resonant transmission near nonrobust periodic slab modes," Phys. Rev. E **71**, 026611 (2005).

[21] S. Shipman and H. Tu, "Total resonant transmission and reflection by periodic structures," SIAM J. Appl. Math. **72**, 216–239 (2012).

[22] Y. Huang and Y. Y. Lu, "Scattering from periodic arrays of cylinders by Dirichlet-to-Neumann maps," Journal of Lightwave Technology **24**, 3448-3453 (2006).

[23] J. Yuan and Y. Y. Lu, "Photonic bandgap calculations using Dirichlet-to-Neumann maps," J. Opt. Soc. Am. A **23**, 3217-3222 (2006).

[24] L. N. Trefethen and D. Bau, Numerical Linear Algebra (Society of Industrial and Applied Mathematics, 1997).

[25] D. V. Evans, M. Levitin, and D. Vassiliev, "Existence theorems for trapped modes," J. Fluid Mech. **261**, 21-31 (1994).

[26] M. S. Birman and M. Z. Solomjak, Spectral Theory of Self-Adjoint Operators in Hilbert Space (Springer, 1987).